# COMPONENT MODE SYNTHESIS

# OF SPACE STATION FREEDOM USING

# MSC/NASTRAN SUPERELEMENT ARCHITECTURE

*Steve Del Basso*
*Sudeep Singh*
*Grumman Space Station Engineering And Integration Contractor*

*Alan J. Lindenmoyer*
*NASA Space Station Freedom Program Office*

## ABSTRACT

The generation of a Space Station Freedom system structural model for on-orbit loads analysis presents an integration challenge. With four prime contractors and three international partners involved, the methodology employed needs to be able to handle a variety of component model representations, and still satisfy all the traditional analysis demands. An approach, which minimizes software development and offers considerable flexibility, relies on the superelement solution sequence of MSC/NASTRAN. Component models can be transferred as physical mass and stiffness matrices, NASTRAN bulk data, or in a generalized, reduced state such as Craig-Bampton transformed mass and stiffness matrices. These are then coupled within MSC/NASTRAN from which the synthesized system modes are obtained. Two such sets of system modes were developed in this study. In one case, component models were derived from an existing system finite element model of the Permanent Manned Capability configuration. This provided a test bed for validation. The other system modes were also for the Permanent Manned Capability configuration, but these were based on preliminary contractor models. In both instances, the approach taken proved effective.

## INTRODUCTION

Space Station Freedom (SSF) is an international collaboration organized to establish a thirty year human presence in space. Figure 1 depicts the Assembly Complete (AC) configuration which is expected to be built before the end of this century. The construction of this 590000 pound structure, as now planned, requires 29 Space Transportation System (STS) flights. It stands 493 feet from starboard truss end to port truss end with 244 foot photovoltaic (PV) array wings spanning the other dimensions.

Four prime United States contractors, organized by work package, and three international partners are contributing to Space Station Freedom's design. Both the Europeans and Japanese are providing pressurized laboratory modules, which are connected to the U.S. laboratory and habitat modules by two pressurized nodes. These components, along with another pair of nodes at the opposite end of the U.S. modules, constitute the principal elements of the module cluster which is the life-supporting core of the space station. All U.S. pressurized volumes, nodes included, with the exception of the airlock, are the responsibility of the Work Package 1 (WP1) prime contractor. The airlock, along with the truss structure and many of the station's system level functions, are supplied by Work Package 2 (WP2). Attached payloads to the truss are the responsibility of Work Package 3 (WP3), and the power generation activity has been assigned to the Work Package 4 prime contractor. A remote manipulator arm with various special purpose tools is to be delivered by the Canadian Space Agency.

As witnessed in the previous paragraph, one of the program challenges will be the successful integration of such a large number of independent and diverse participants. This concern surfaces at the structural analysis level, and in particular in the on-orbit loads area. On-orbit loads need to be determined not only for the final AC configuration, but also for each of the intermediate stages, any growth scenarios or post-AC variations, and at any critical phase of assembly. There are internal forces and dynamic clearances to be determined from such significant events as module berthing, STS docking, STS plume impingement, and reaction control system (RCS) jet firings. Acceleration response predictions must extend into the microgravity range ($10^{-6}$ g's) in support of material science research which requires consideration of almost any disturbance such as crew motion and centrifuge operation. Further, the system structural dynamic model must also be available for flight control analyses in both open and closed loop simulations.

Given the scope of the problem, and the desire to not introduce any unnecessary constraints upon the team members, the inherent capabilites of MSC/NASTRAN, combined with its user programming power, made MSC/NASTRAN a logical choice for system model generation. MSC/NASTRAN can accept component structural dynamic models in physical mass and stiffness matrix form, as NASTRAN bulk data, or in some generalized, reduced state, such as Craig-Bampton (Reference 1) transformed mass and stiffness matrices. Once in NASTRAN, generalized models can be developed from physical models, and standard component model checks may be performed. The component modal synthesis is then implemented by a standard MSC/NASTRAN superelement modal analysis solution sequence, obviating the need for the analyst to formulate the coupling transformation and produce the coupled system mass and stiffness. An additional benefit, is the relative simplicity by which component models can be rotated and/or duplicated. This permits the use of one component model at multiple locations either simultaneously or whenever the configuration calls for its change in position, provided the boundary conditions are correct.

At present, component structural models are transferred either as physical NASTRAN models or Craig-Bampton models. The similarity between the Craig-Bampton formulation and MSC/NASTRAN's superelement architecture will be discussed, and the coupling procedure outlined. Results from two cases examined are presented. In the first case, Craig-Bampton component models were derived from an existing system level beam model from which results could be compared. In the other case, preliminary, detailed contractor models were combined. This is followed by the recommendations and conclusions of the study.

## COMPONENT MODE SYNTHESIS

The generation of system modes from component modes, typically begins with the transformation of the component physical model into a reduced model which may include physical as well as modal degrees of freedom (dofs). In this study, Craig-Bampton component models were used. Equation 1 contains the Craig-Bampton transformation which is applied to the component's free physical mass and stiffness matrices, partitioned into boundary (b) and interior (i) dof groupings.

$$\begin{bmatrix} X_b \\ X_i \end{bmatrix} = \begin{bmatrix} I & 0 \\ \phi_c & \phi_n \end{bmatrix} \begin{bmatrix} X_b \\ q \end{bmatrix} \tag{1}$$

$X_b$ = displacement of physical dofs at the boundary
$X_i$ = displacement of physical dofs in the interior
$q$ = displacement of modal dofs
$\phi_c$ = constraint modes (interior displacements due to unit boundary displacements, applied one at a time with the other boundary dofs constrained)
$\phi_n$ = normal modes with the boundary dofs constrained

The resulting, transformed mass and stiffness matrices take the following form:

$$[m] = \begin{bmatrix} M_{bb}+M_{bi}\phi_c+\phi_c^t M_{bi}^t+\phi_c^t M_{ii}\phi_c & M_{bi}\phi_n+\phi_c^t M_{ii}\phi_n \\ \text{sym} & \phi_n^t M_{ii}\phi_n \end{bmatrix}$$

$$[k] = \begin{bmatrix} K_{bb}+K_{bi}\phi_c & 0 \\ 0 & \phi_n^t K_{ii}\phi_n \end{bmatrix} \tag{2}$$

If the component model needs to be reoriented for compliance with the system configuration and/or coordinates or for duplication, the mass and stiffness terms associated with the physical boundary dofs must be appropriately transformed. Such a coordinate transformation requires the development of the 3x3 direction cosine matrix between the unit vectors of the two coordinate systems, and then its proper incorporation into a boundary dof size matrix which is to pre and post multiply the existing component terms.

Once all component models are correctly located and in a common coordinate system, the component mass and stiffness terms can be assembled into an uncoupled system mass and stiffness matrix. This is accomplished by simply stacking each of the component model terms along the diagonal. For example, for a two component system, where the normal modes have been mass normalized, the uncoupled system stiffness matrix appears as:

$$[K_s] = \begin{bmatrix} K_{bb1}+K_{bi1}\phi_{c1} & 0 & & \\ 0 & \omega_{n1}^2 & \multicolumn{2}{c}{\varnothing} \\ \multicolumn{2}{c}{\varnothing} & K_{bb2}+K_{bi2}\phi_{c2} & 0 \\ & & 0 & \omega_{n2}^2 \end{bmatrix} \tag{3}$$

What remains is the construction of a coupling matrix which when used to pre and post multiply the uncoupled system matrices yields the coupled matrices from which system eigenvalues and eigenvectors can be extracted. The coupling is based on some type of constraint equation between dofs within the individual components. For the two component example of equation (3), a constraint may be introduced which equates the boundary displacements of component 2 to certain interior displacements of component 1. Since component 1's interior dofs have been reduced from the problem, its boundary and modal dofs are used with the appropriate transformation terms as the independent dofs in the constraint equation. In matrix form, the equations are:

$$\begin{bmatrix} X_{b1} \\ q_1 \\ X_{b2} \\ q_2 \end{bmatrix} = \begin{bmatrix} I & 0 & 0 \\ 0 & I & 0 \\ \bar{\phi}_{c1} & \bar{\phi}_{n1} & 0 \\ 0 & 0 & I \end{bmatrix} \begin{bmatrix} X_{b1} \\ q_1 \\ q_2 \end{bmatrix} \tag{4}$$

$\bar{\phi}_{c1}$ = those dofs of component 1's constraint modes which correspond to component 2's boundary dofs

$\bar{\phi}_{n1}$ = those dofs of component 1's normal modes which correspond to component 2's boundary dofs

Of course, the component mode synthesis outline presented here is but one of many possible approaches. It is intended to show the basic steps in the procedure for comparison with the MSC/NASTRAN superelement method.

MSC/NASTRAN SUPERELEMENT ARCHITECTURE

An 'internal' MSC/NASTRAN superelement is developed from an existing MSC/NASTRAN physical finite element bulk data set via standard solution sequences. The finite element model (FEM) is organized into a set of analysis dofs (a) and internal dofs (o) (Reference 2) with the aim of performing any further computations solely on the reduced analysis set. The analysis dofs may consist of physical boundary dofs (t), and, in the case of a dynamic formulation, of generalized, modal dofs (q). The following transformation relates these quantities:

$$[u_o] = \begin{bmatrix} G_{ot} & G_{oq} \end{bmatrix} \begin{bmatrix} u_t \\ u_q \end{bmatrix} \qquad (5)$$

Based on equation 5, reduced mass and stiffness matrices are generated for the superelement, and these are stored along with a complete information package of the initial FEM on an associated data base.

Examination of equations 5 and the lower partition of equation 1 reveal a similarity in the transformations, where $G_{ot}$ corresponds to $\phi_c$, and $G_{oq}$ to $\phi_n$ . Thus, the superelement mass and stiffness matrices can represent reduced Craig-Bampton mass and stiffness matrices.

A superelement data base contains two analysis set (a) sized matrices for both the reduced mass and stiffness. These are labeled MAA and MLAA for the mass, and KAA and KLAA for the stiffness. The MAA and KAA blocks carry the physical boundary dof (t) data in the appropriate matrix positions, while the MLAA and KLAA possess the t-q coupling and generalized dof (q) terms, again, at the appropriate matrix positions. In a normal modes solution, the MAA and MLAA are combined as are the KAA and KLAA. This permits one to create a superelement data base by simply assembling the Craig-Bampton matrix elements into MAA and KAA matrices which may be assigned a qualifier to designate its superelement id number.

With such a data base established for each Craig-Bampton model, the remaining tasks in a component mode synthesis procedure may now be all efficiently processed within an MSC/NASTRAN 'residual' run. The Craig-Bampton superelement data base is identified as an 'external' superelement with each of its dofs accounted for on a 'CSUPER' input card. The physical dofs may be associated with grids or scaler points, and the generalized dofs with scaler points. The boundary grids must be defined in this 'residual' run, and these may be utilized to perform any needed coordinate transformations. This is accomplished by specifying an output coordinate system on the 'GRID' input card different from the basic system in which all the grids are expressed. Duplicate superelements can be formed by copying a data base, and introducing a unique id. Any reorientation is then handled as a coordinate transformation.

Coupling of the component models, superelements, is executed with standard MSC/NASTRAN commands. One can use 'RBAR' type elements, or assign multi-point constraints (MPCs) with the 'MPC' input card. Physical FEMs may also be part of the 'residual' run or they may be treated as 'internal' superelements.

Once all the components have been assembled and coupled, the system modes are obtained and output onto a superelement '0' data base. For 'internal' superelements, standard MSC/NASTRAN solution sequences perform the backsubstitution. Equation 5 is employed to go from the system modes in the analysis dofs, to physical system modes in the boundary and internal dofs. For 'external' superelements, Direct Matrix Abstraction Programming (DMAP) is available within MSC/NASTRAN to execute this step which makes use of the transformation shown in equation 1. Particular attention must be given to all components which have undergone coordinate transformations to assure accurate results.

## COMPONENT MODE SYNTHESIS WITH SYSTEM FEM

The feasibility of using MSC/NASTRAN for component mode synthesis was initially demonstrated by two sample problems. A 3 dof, three mass problem, allowed comparison with hand calculations, and an 18 dof 'L' shaped two beam problem served as the first FEM example. After both results proved satisfactory, attention was given to the SSF Preliminary Loads Analysis (PLA) Permanent Manned Capability (PMC) FEM.

The PLA activity was initiated by the NASA SSF Program Office to provide typical on-orbit loads and dynamic responses to start preliminary design (Reference 3). These analyses were based on system level FEMs developed by the integrating contractor. One such model is of the PMC configuration which is shown in Figure 2. The PMC stage includes only half of AC's power generation capacity, lacking the outboard PV wings and the accompanying truss bays on both starboard and port sides. In addition, the European and Japanese modules have not yet been delivered. The total PMC FEM weight is 398487 (Lbm), and it contains some 1208 elastic elements and 2802 dofs.

The PLA PMC FEM provided an opportunity to evaluate the proposed component mode synthesis (CMS) procedure on a 'real' problem which had been independently solved. First, the system PMC FEM was solved for normal modes. This was done to confirm that the model in hand was identical to the model documented in reference 3, and to establish a data base for later analysis. The PMC FEM was then dissected into five separate FEMs:

(1) Starboard, forward PV array;
(2) Starboard truss, outboard of the alpha joint;
(3) Port truss, outboard of the alpha joint;
(4) Module cluster;
(5) Center truss inboard of the alpha joints plus the alpha joints themselves.

These components were then formulated into Craig-Bampton models by combining DMAP alters with MSC/NASTRAN version 65C solution 3. Pertinent component model properties are listed in Table 1. In all cases but the arrays and center truss, component modes to 10 hertz were retained to provide sufficent data to recover system modes up to 5 hertz. The array models kept modes to 5 hertz, and a default 100 mode per component limit truncated the center truss at 7.1 hertz.

Before executing the 'residual' run for system modes, the component models underwent a series of checks, and a superelement data base was created for each containing only MAA and KAA. Three copies of the starboard, forward PV array superelement data base were made to account for the starboard, aft PV array, and the two port side arrays. The only difference among the four was the superelement id number assigned to the matrices. Standard checks performed on the Craig-Bampton matrix partitions included:

(1) Boundary stiffness equilibrium checks;
(2) Boundary mass check, where the boundary mass matrix is rigid-body transformed to a selected 6 dof reference grid, and the resulting terms compared to the FEM mass matrix about that grid;
(3) Constraint mode check, where the constraint modes are used to transform a rigid body transformation matrix from the boundary dofs to the internal dofs which is then compared to an independently generated rigid body transformation matrix associated with those same internal dofs;
(4) Modal effective weight calculation based on the coupling mass matrix term. This not only provides the modal mass distribution among modes and the coordinate direction in which the mass is active, but also gives an indication if the coupling term is properly functioning. A comparison with a kinetic energy check should show similar trends;
(5) Kinetic energy check, based on physical mass and normal modes, characterizes the modes, and supports the modal effective weight check;

A final check was then performed on the assembled Craig-Bampton mass and stiffness matrices which are representative of a free structure. Normal modes were extracted from the MAA and KAA matrices, and examined for rigid body modes and reasonableness of flexible modes. This was also performed on the 'internal' superelement which was processed as an 'external' superelement after adding its MAA and MLAA, and KAA and KLAA blocks, and storing these as MAA and KAA on a new data base. In all these cases, user DMAP was implemented to perform the checks. In addition, a MSC/NASTRAN supplied DMAP alter was applied to the 'internal' superelement run which computed the equilibrium and mass checks for that particular case (Reference 4).

Once all the component models passed these checks, the 'residual' run was made to determine the system modes. There were eight input superelement data bases which provided the MAA and KAA for each of the components. The starboard aft PV array, and the port aft PV array boundary grids were assigned output coordinate systems which were rotated from the basic. This technique transformed the mass and stiffness terms connected to the boundary from the forward orientation in which they were developed, to the aft orientation. The grid order on the 'CSUPER' card must also take such rotations into account. 'RBAR' elements were used to couple the components at all interfaces except the module cluster to center truss. Here, 'MPC's were used to equate displacements on a dof by dof basis. This was necessitated by the module cluster boundary dof set which included only the kinematic attachment dofs.

Table 2 compares the system mass properties between the PLA PMC finite element model and its CMS model derivative. Table 3 compares the first 24 modal frequencies. In both instances, the agreement is good. The CMS version has 92 system modes to 5 hertz, while the finite element model produced 93. This may be due to the truncation of PV arrray component modes above 5 hertz, or center truss modes above 7.1 hertz. Note, that the system modes constitute a transformation from the system modal coordinates to the boundary and generalized component dofs contained in the 'residual' run. Thus the system modes, in themselves, present valuable information regarding component mode participation per system mode.

In order to plot the system modes, and to make them available for further analyses based on the physical FEM, the system modes need to be transformed into the component interior dofs as well. This was accomplished by DMAP coding which made use of the Craig-Bampton component data base or the 'internal' superelement data base within which the original transformations were saved (equations 1 or 5). The NASTRAN 'PLOT' module was then called to generate the plots, and the same data was output for Structural Dynamics Research Corporation (SDRC)/SUPERTAB post-processing. Spatial location and connectivity for plotting was obtained from the FEM grids and elements. If these are not available, plotting grids and elements would have to be created. Components which were rotated but used an unrotated Craig-Bampton transformation to obtain their interior dofs, had to have this portion of their physical system modes undergo a coordinate transformation prior to plotting. This was readily handled by the MSC/NASTRAN 'VECPLOT' module. In all of these matrix manipulations, it is crucial to control the dof order so that the correct computation is performed with a minimal amount of effort. For simplicity, all calculations in this study were with matrices in 'external' order, i.e. ascending grid number. Figure 3 includes plots of the first system truss bending mode as produced by the PLA PMC FEM and its CMS equivalent. The CMS mode is shown on a component basis.

The CMS system modes were also compared to the FEM system modes by a 'dot' product check on the component level. The output of the 'dot' product check may be conceptualized as the cosine of the angle between two vectors. If the mode shapes are identical, the angle is zero and the dot product value is 1. The DMAP coding followed the classical definition:

$$\cos\theta = \frac{\bar{A} \bullet \bar{B}}{|A|\,|B|} \tag{6}$$

Dot products of the PV array, module cluster, and center truss components resulted in diagonal values of 1, consistently through the truss second bending mode. Component kinetic energies were also calculated for the system modes since their physical mass matrices were available. This aids the system mode identification process.

## COMPONENT MODE SYNTHESIS WITH PRELIMINARY WORK PACKAGE MODELS

Table 4 lists the preliminary work package models delivered to date. Components are identifed with regard to work package number, model type (Craig-Bampton or FEM), weight, and, in the case of Craig-Bampton models, frequency content. Typical components, as obtained from contractor documentation are displayed in Figure 4. Note, that these component weights do not, in general, agree with those in the PMC FEM previously discussed. At minimum, each Craig-Bampton component was checked for its free-free modal content prior to use in the 'residual' run.

The PLA PMC configuration was chosen as the initial system for development so that comparisons to the earlier FEM effort could be made. Since the module cluster itself consists of 9 WP1 components, and 3 WP2 components, the synthesis of a module cluster component model was a logical first step. By including only the WP1 components in a 'first pass' run, comparisons could be made with WP1 computed results. These agreed well in both frequency and mass property. There were 15 modes to 5 hertz, including 6 rigid body modes. The first flexible mode occurred at 0.65 hertz.

A system model was assembled with the WP4 PV array and truss/EPS/IEA components; the WP2 alpha joint and station radiator models; and with the center truss and module cluster derived from the PLA FEM. Results from the system run are presented in Table 5. The first truss bending mode now occurs at mode 51 at 0.184 hertz rather than at the FEM's mode 19 which is at 0.183 hertz. This difference in mode number is attributed to the increased modal content of the work package component models. While the FEM contained only 93 modes below 5.0 hertz, this version of PMC had 267 modes below 5.0 hertz with 125 modes below 0.5 hertz. This is indicative of the high modal density one can expect in the SSF load cycle models.

## RECOMMENDATIONS/CONCLUSIONS

The component mode synthesis procedure, based on MSC/NASTRAN superelement architecture, is a viable technique for system model generation. This approach minimizes code development time, and offers the benefits of MSC/NASTRAN for component model orientation, coupling, and eigen-problem solution.

As a minimum check, the rigid body modes of a Craig-Bampton component model should be determined and evaluated. The selection of component modes to retain in component mode synthesis is also of importance. Consideration should be given to frequency content, modal effective mass, and input/output sensitivities. 'Rules of thumb' suggest a frequency content which is1.5 to 2.0 times greater than the system frequency range of interest.

Future products will include system level plots of the CMS generated modes to complement the current 'by component' plots, and self/ cross orthogonality check outputs where applicable. The entire procedure needs to be exercised with a component model which carries residual degrees of freedom to assure this capability. Eventually, the procedure must catch up with MSC and be transfered into version 66.

## REFERENCES


1. Craig, R.R., and Bampton, M.C.C., "Coupling of Substructures for Dynamic Analyses", AIAA Journal, Volume 3, No. 7, July 1968.

2. MSC/NASTRAN Application Manual, "Generalized Dynamic Reduction", The MacNeal-Schwendler Corporation, Los Angeles, California, April 1981.

3. Barickman, K., Draper, C., Havelka, J., Kim, H.M., Shein, S.L., and Partin, J., "Preliminary Loads Analysis", McDonnell Douglas Space Systems Company Space Station Division, Houston, Texas, February 1989.

4. Muskivitch, J.C., "MSC/NASTRAN Superelement Analysis", The MacNeal-Schwendler Corporation Eastern Engineering Services Office, Rockville, Maryland, February 1988.

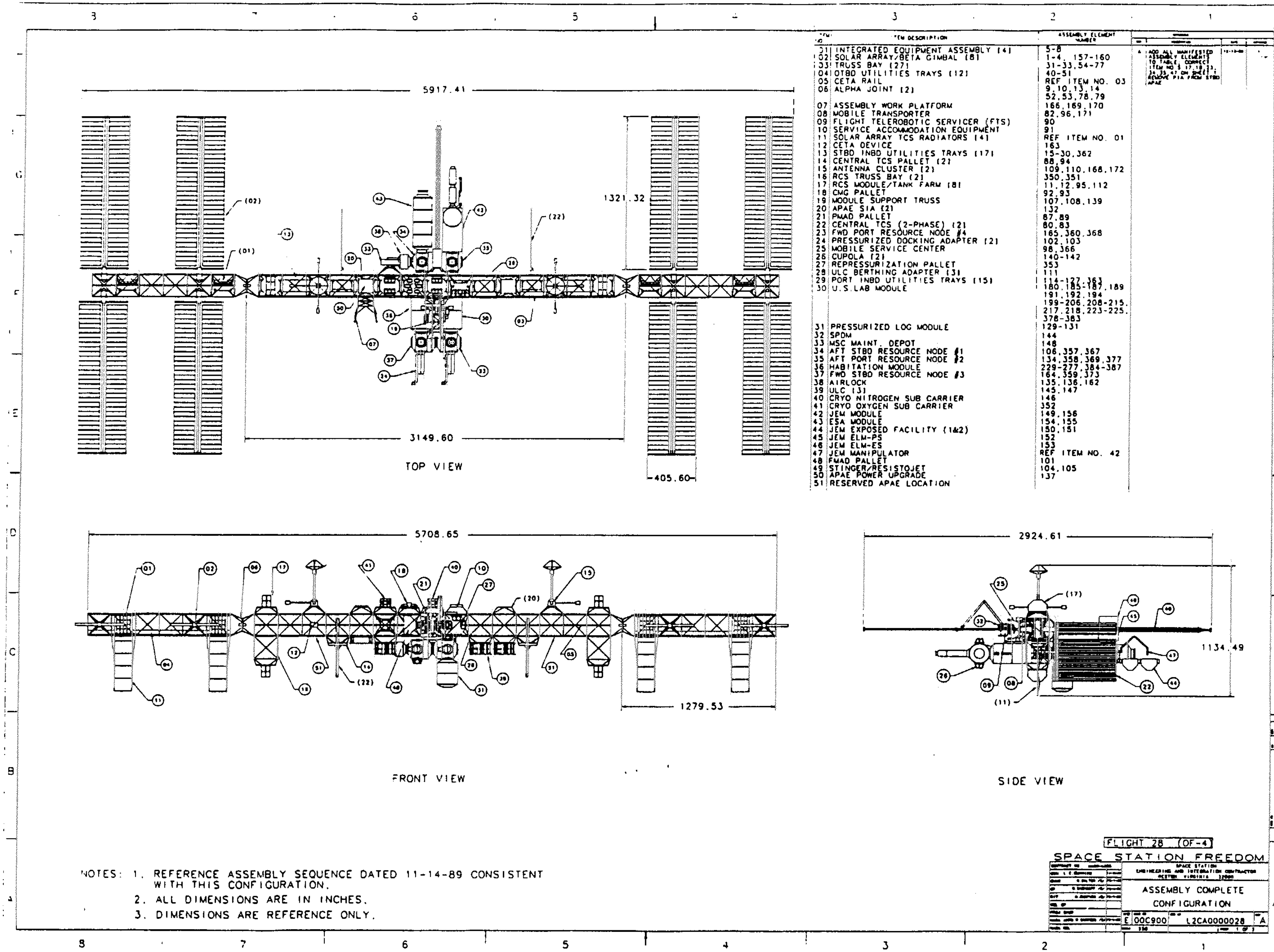


| ITEM NO | ITEM DESCRIPTION | ASSEMBLY ELEMENT NUMBER |
|---|---|---|
| 01 | INTEGRATED EQUIPMENT ASSEMBLY (4) | 5-8 |
| 02 | SOLAR ARRAY/BETA GIMBAL (8) | 1-4, 157-160 |
| 03 | TRUSS BAY (27) | 31-33,54-77 |
| 04 | OTBD UTILITIES TRAYS (12) | 40-51 |
| 05 | CETA RAIL | REF ITEM NO. 03 |
| 06 | ALPHA JOINT (2) | 9,10,13,14 52,53,78,79 |
| 07 | ASSEMBLY WORK PLATFORM | 166,169,170 |
| 08 | MOBILE TRANSPORTER | 82,96,171 |
| 09 | FLIGHT TELEROBOTIC SERVICER (FTS) | 90 |
| 10 | SERVICE ACCOMMODATION EQUIPMENT | 91 |
| 11 | SOLAR ARRAY TCS RADIATORS (4) | REF ITEM NO. 01 |
| 12 | CETA DEVICE | 163 |
| 13 | STBD INBD UTILITIES TRAYS (17) | 15-30,362 |
| 14 | CENTRAL TCS PALLET (2) | 88,94 |
| 15 | ANTENNA CLUSTER (2) | 109,110,168,172 |
| 16 | RCS TRUSS BAY (2) | 350,351 |
| 17 | RCS MODULE/TANK FARM (8) | 11,12,95,112 |
| 18 | CMG PALLET | 92,93 |
| 19 | MODULE SUPPORT TRUSS | 107,108,139 |
| 20 | APAE SIA (2) | 132 |
| 21 | PMAD PALLET | 87,89 |
| 22 | CENTRAL TCS (2-PHASE) (2) | 80,83 |
| 23 | FWD PORT RESOURCE NODE #4 | 165,360,368 |
| 24 | PRESSURIZED DOCKING ADAPTER (2) | 102,103 |
| 25 | MOBILE SERVICE CENTER | 98,366 |
| 26 | CUPOLA (2) | 140-142 |
| 27 | REPRESSURIZATION PALLET | 353 |
| 28 | ULC BERTHING ADAPTER (3) | 111 |
| 29 | PORT INBD UTILITIES TRAYS (15) | 114-127,363 |
| 30 | U.S. LAB MODULE | 180,185-187,189 191,192,194 199-206,208-215, 217,218,223-225, 378-383 |
| 31 | PRESSURIZED LOG MODULE | 129-131 |
| 32 | SPDM | 144 |
| 33 | MSC MAINT. DEPOT | 148 |
| 34 | AFT STBD RESOURCE NODE #1 | 106,357,367 |
| 35 | AFT PORT RESOURCE NODE #2 | 134,358,369,377 |
| 36 | HABITATION MODULE | 229-277,384-387 |
| 37 | FWD STBD RESOURCE NODE #3 | 164,359,373 |
| 38 | AIRLOCK | 135,136,162 |
| 39 | ULC (3) | 145,147 |
| 40 | CRYO NITROGEN SUB CARRIER | 146 |
| 41 | CRYO OXYGEN SUB CARRIER | 352 |
| 42 | JEM MODULE | 149,156 |
| 43 | ESA MODULE | 154,155 |
| 44 | JEM EXPOSED FACILITY (1&2) | 150,151 |
| 45 | JEM ELM-PS | 152 |
| 46 | JEM ELM-ES | 153 |
| 47 | JEM MANIPULATOR | REF ITEM NO. 42 |
| 48 | FMAD PALLET | 101 |
| 49 | STINGER/RESISTOJET | 104,105 |
| 50 | APAE POWER UPGRADE | 137 |
| 51 | RESERVED APAE LOCATION | |

Figure 1

Space Station Freedom Assembly Complete Configuration Solid Model

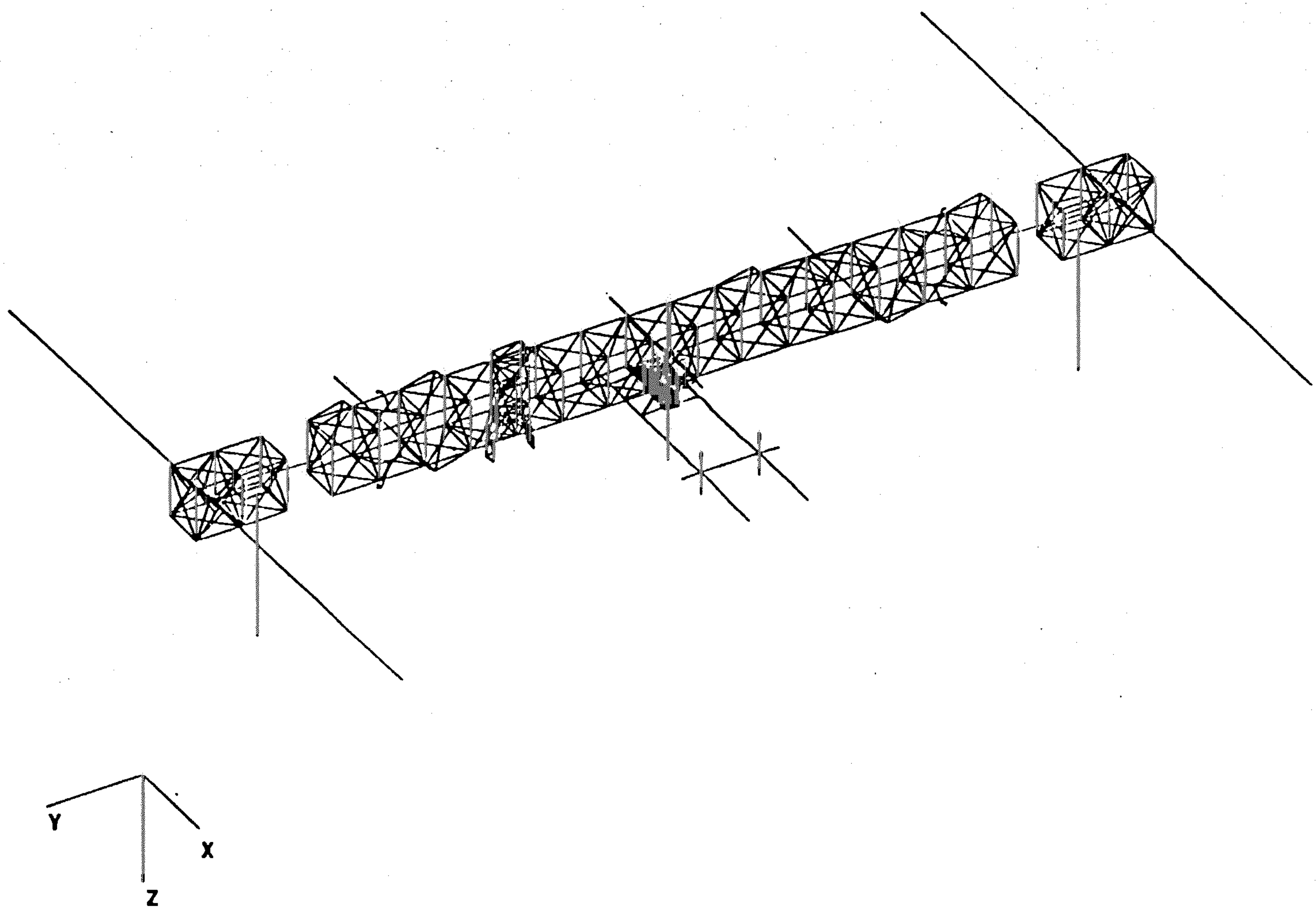


Figure 2

PLA Permanent Manned Capability Configuration Finite Element Model

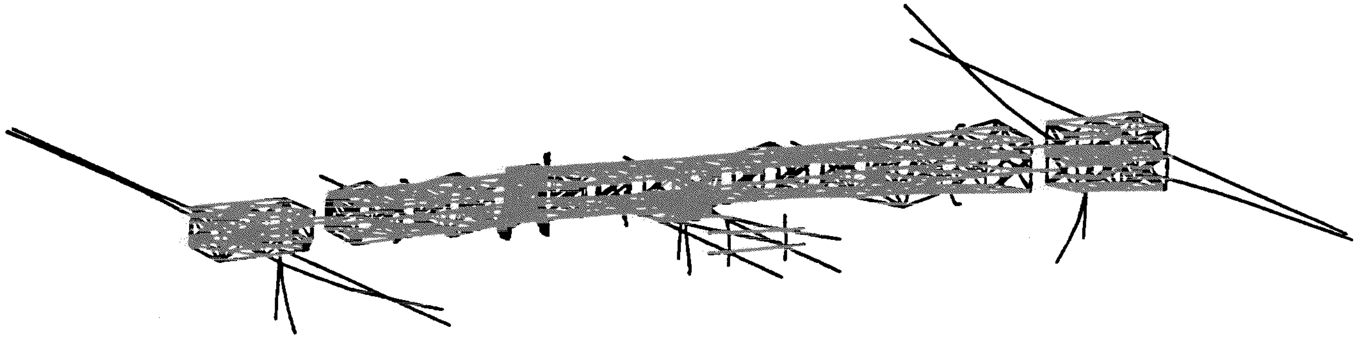

Truss Bending Mode of the PLA FEM Model ( f = .183 hz)

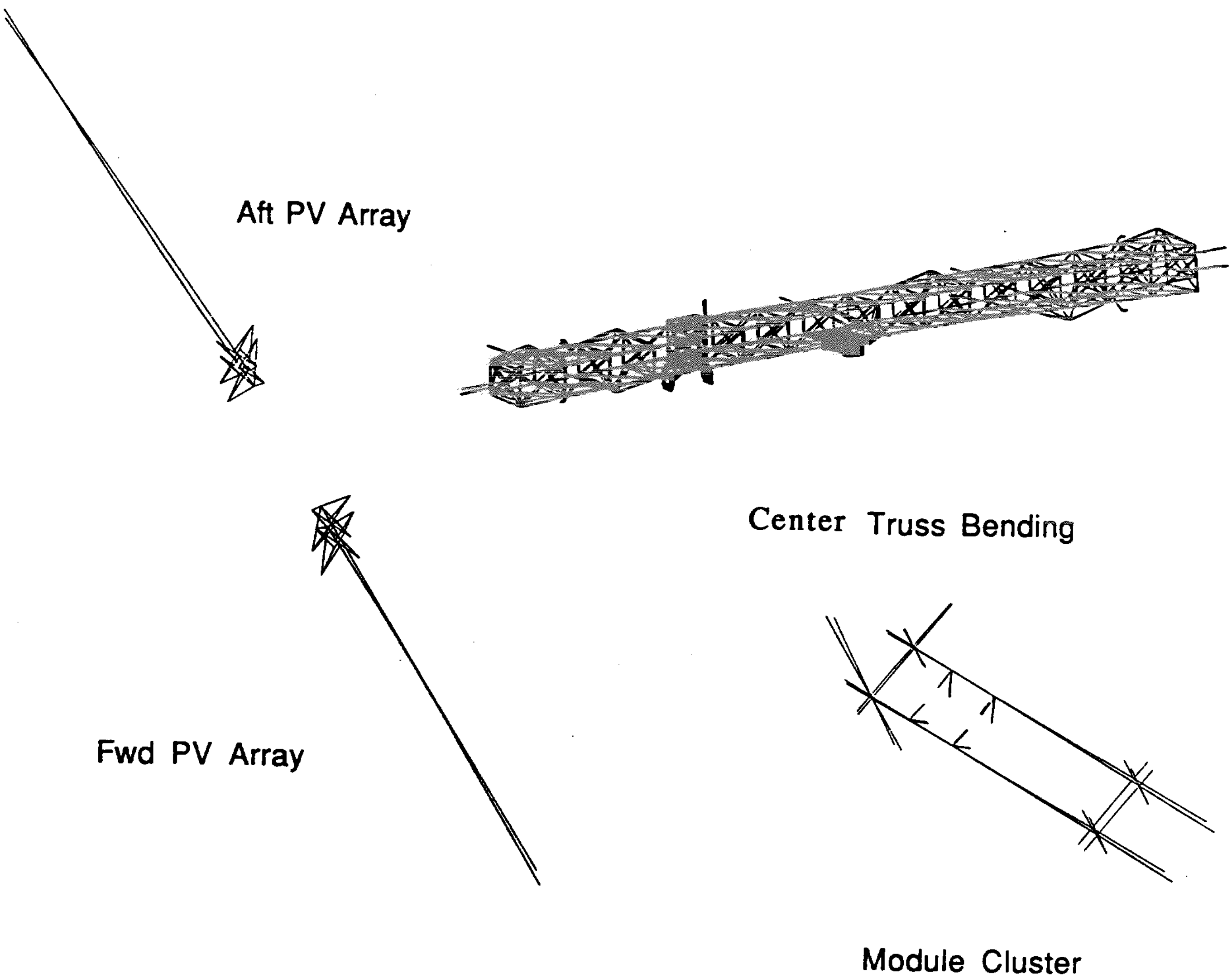


Truss Bending Mode of the CMS Model ( f = .183 hz)

Figure 3

Mode Shape Comparison Between PLA FEM and CMS Models

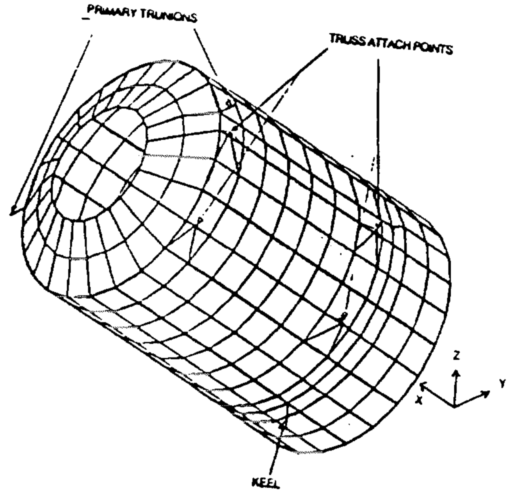


Lab Model

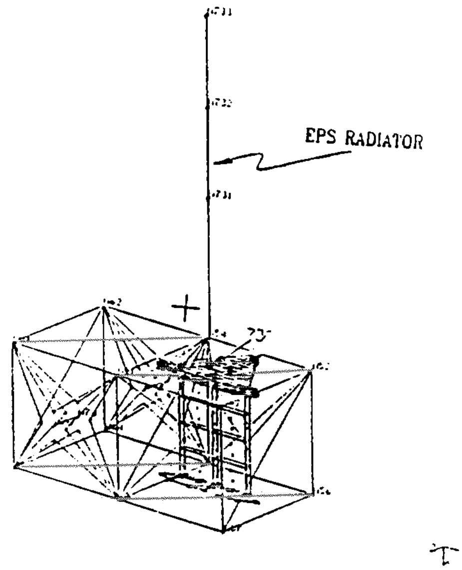


Truss+IEA + EPS Rad.

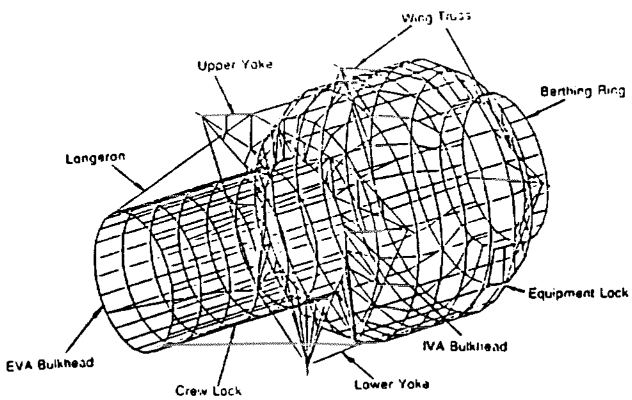


Airlock

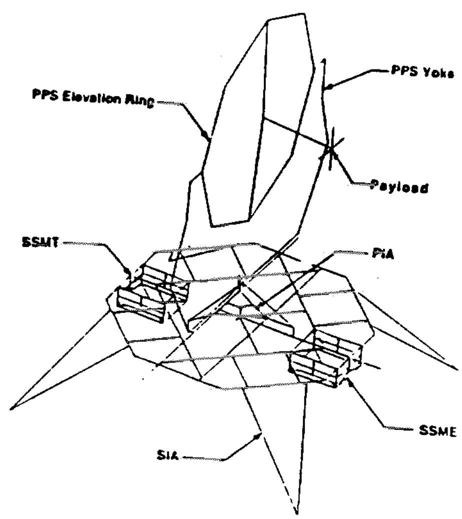


Attached Payload

Figure 4

Typical Work Package Models

**Table 1**

**Model Properties for Components Derived from PLA**

**PMC Finite Element Model**

| Component Model | Boundary DOFS | Interior DOFS | Mass (lbm) | Modes (0-5 hz) | No. of Modes to 10 hz |
|---|---|---|---|---|---|
| 1. Stbd, Fwd PV Array | 24 | 78 | 2008 | .1005<br>.1385<br>1.5484<br>2.0160<br>4.4824 | (not calculated) |
| 2. Stbd Truss, Outbd of Alpha Joint | 54 | 24 | 10386 | .0947<br>.5948<br>.9120<br>1.7357<br>2.0298<br>4.4956 | 8 |
| 3. Port Truss, Outbd of Alpha Joint | 54 | 24 | 10347 | .0947<br>.5948<br>.9120<br>1.7357<br>2.0298<br>4.4958 | 8 |
| 4. Module Cluster | 16 | 326 | 247,143 | .5839<br>.9456<br>2.0004<br>2.2282<br>2.9848<br>3.7754<br>3.9500<br>4.6478 | 13 |
| 5. Center Truss Inbd of Alpha Joint + Alpha Joint | 60 | 1300 | 122,471 | .1511<br>.1511<br>.1577<br>.2070<br>.2654<br>.5480<br>.5496<br>.6781<br>.7875<br>.9363<br>(36 modes to 5 hz) | 100<br>(to 7.1 hz) |

**Table 3**

**System Modes Comparison Between PLA FEM and CMS Models**

| Mode No. | Frequency PMC-FEM | Frequency PMC-CMS | Description |
|---|---|---|---|
| 1 | 5.18678E-07 | 6.52340E-07 | Rigid Body |
| 2 | 3.84785E-07 | 2.31784E-07 | Rigid Body |
| 3 | 9.94193E-08 | 2.14465E-07 | Rigid Body |
| 4 | 1.90776E-07 | 3.45224E-07 | Rigid Body |
| 5 | 2.36437E-07 | 5.23094E-07 | Rigid Body |
| 6 | 2.89910E-07 | 6.19393E-07 | Rigid Body |
| 7 | 9.42507E-02 | 9.42508E-02 | EPS Radiator |
| 8 | 9.48161E-02 | 9.48162E-02 | EPD Radiator |
| 9 | 9.66451E-02 | 9.66450E-02 | PV Array |
| 10 | 1.00078E-01 | 1.00079E-01 | PV Array |
| 11 | 1.00570E-01 | 1.00570E-01 | PV Array |
| 12 | 1.02642E-01 | 1.02643E-01 | PV Array |
| 13 | 1.35421E-01 | 1.35422E-01 | PV Array |
| 14 | 1.38869E-01 | 1.38869E-01 | PV Array |
| 15 | 1.39407E-01 | 1.39408E-01 | PV Array |
| 16 | 1.39803E-01 | 1.39804E-01 | PV Array |
| 17 | 1.50553E-01 | 1.50554E-01 | Station Radiator |
| 18 | 1.52486E-01 | 1.52487E-01 | Station Radiator |
| 19 | 1.83030E-01 | 1.83039E-01 | Truss Bending+ |
| 20 | 2.12776E-01 | 2.12789E-01 | Truss Bending+ |
| 21 | 2.27838E-01 | 2.27871E-01 | Truss Bending+ |
| 22 | 3.03957E-01 | 3.04005E-01 | Truss Bending+ |
| 23 | 3.26355E-01 | 3.26372E-01 | Truss Bending+ |
| 24 | 3.43074E-01 | 3.43108E-01 | Truss Bending+ |

**TABLE 2**

**Mass Property Comparison Between FEM and CMS Models**

| | PMC FEM | PMC CMS MODEL |
|---|---|---|
| Mass (lbm) | 398571.03 | 398470.00 |
| Ixx (lbm-in2) | 2.1196E11 | 2.1198E11 |
| Iyy | 7.4496E10 | 7.4497E10 |
| Izz | 2.1736E11 | 2.1731E11 |
| Ixy | 1.2806E9 | 1.2806E8 |
| Ixz | 4.3091E9 | 4.3091E9 |
| Iyz | 8.6375E8 | 8.6375E8 |
| CGx (in) | 32.9745 | 33.051 |
| CGy | 66.8267 | 66.830 |
| CGz | 120.381 | 120.385 |

| Table 4 | | | | | | |
|---|---|---|---|---|---|---|
| **Description of Contractor Models** | | | | | | |
| Component Name | Contractor | Type CB/FEM | Weight (lbm) | DOF Modal | DOF Phy | Frequency Range (hz) |
| 1. Cupola | WP1 | CB | 3,131 | 3 | 144 | 40.6 - 46.6 |
| 2. U S Lab (fully outfitted) | WP1 | CB | 71,640 | 1 | 343 | 9.05 |
| 3. U S Hab (fully outfitted) | WP1 | CB | 37,952 | 2 | 342 | 8.23 - 8.92 |
| 4. Node | WP1 | CB | 21,570 | 69 | 912 | 17.9 - 69.14 |
| 5. Press. Log | WP1 | CB | 26,177 | 3 | 144 | 1.75 - 8.30 |
| 6. PV Array | WP4 | CB | 1,441 | 12 | 33 | .110 - 4.7 |
| 7. Outbd Truss + IEA + EPS Rad. | WP4 | CB | 13,123 | 72 | 9 | .095 - 14.0 |
| 8. SSF Truss | WP2 | FEM | 17,000 | | | |
| 9. TCS Radiators | WP2 | CB,FEM | 4,371 | 34 | 6 | .11 - 4.7 |
| 10. Docking Mast | WP2 | FEM | 2,270 | | | |
| 11. Alpha Joint | WP2 | FEM | 598 | | | |
| 12. Universal Pallets | WP2 | FEM | 6,000 | | | |
| 13. Mobile Transp. | WP2 | FEM | 3,823 | | | |
| 14. Deployable Booms | WP2 | FEM | 1,158 | | | |
| 15. Module to Truss | WP2 | FEM | 368 | | | |
| 16. Airlock | WP2 | FEM | 11,932 | | | |
| 17. Unpressurized Log. Element | WP2 | FEM | 10,147 | | | |
| 18. Assembly Work Platform | WP2 | CB,FEM | 1,406 | 34 | 24 | .60 - 4.7 |
| 19.Attached Payloads | WP3 | CB,FEM | | | | |
| Model 1 | | | 16,306 | 6 | 8 | 1.25 - 6.02 |
| Model 2 | | | 8,222 | 4 | 8 | 1.98 - 7.24 |
| Model 3 | | | 8,987 | 4 | 8 | 1.90 - 6.52 |
| Model 4 | | | 25,407 | 6 | 8 | 1.11 - 7.79 |
| Model 5 | | | 22,635 | 6 | 8 | 1.02 - 5.83 |
| 20.ESA Module | ESA | FEM | 61,143 | | | |
| 21.JEM Module | NASDA | FEM | 55,433 | | | |

| Table 5 | | |
|---|---|---|
| **System Modes with Preliminary Contractor Models with PLA Module Cluster** | | |
| | Frequency (hz) | Description |
| Mode No. | PMC-CMS | |
| 1 - 6 | 6.8E-4 - 1.5E-2 | Rigid Body |
| 7 | .095 | Radiator |
| 8 | .095 | Radiator |
| 9 - 34 | .106 -.114 | Radiator and PV array |
| 35 - 50 | .123 - .140 | PV Array |
| 51 | .184 | SS Truss Bending |
| 52 - 55 | .191 -.195 | PV Array |